ISSN 1330–0016
CODEN FIZBE7

THE ^{27}Al(^{14}N, X) REACTION MECHANISMS AT THE 129.3 MeV BOMBARDING ENERGY

GIOVANNI FAZIO, GIORGIO GIARDINA, ROBERTO STURIALE, OLEG YU. GORYUNOV[a] and ANATOLY A. SHVEDOV[a]

Istituto Nazionale di Fisica Nucleare, Sezione di Catania and Dipartimento di Fisica dell'Università di Messina, Salita Sperone 31, 98166 Villaggio Sant'Agata, Messina, Italy
[a] Institute for Nuclear Research, National Academy of Sciences of Ukraine, Prospect Nauki 47, 252028 Kiev, Ukraine

Received 25 September 1996

Revised manuscript received 29 November 1996

UDC 539.17

PACS 25.70.-z

Absolute values of differential cross–sections for the formation of ^{6,7}Li, ^{7,9}Be, ^{10,11}B and ^{12}C nuclei were measured by the ^{14}N + ^{27}Al reaction at 129.3 MeV. The analysis of the inclusive energy spectra and angular distributions shows that the carbon and boron fragment production is well described by the projectile break–up leading to three–body final states reactions, while the lighter fragments are due both to the above–mentioned break–up and the evaporation from the ^{41}Ca compound nucleus.

1. Introduction

The production mechanisms of fragments lighter than projectiles in heavy–ion induced reactions on medium–light target nuclei and their competition are today an open problem. We investigated the ^{27}Al(^{14}N, X) reaction at 129.3 MeV bombarding energy. It has previously been studied at 62 [1] and 116 [2] MeV bombarding energy by the analysis the inclusive energy spectra of reaction products lighter than the projectile. The authors affirm that the experimental data deduced at 62 MeV [1] are well reproduced by two–body final state calculations while the ones at 116 MeV [2] by three–body final state calculations, showing that break–up of the projectile depends on the bombarding energy. The calculations for the 62 MeV reactions were performed by considering the hypothesis that a particle was transferred from the projectile to the target leaving a two–body final state. In the 116 MeV reactions, the target nucleus acts as a spectator that provides the field for the projectile break–up. During the interaction, the target can be excited, remaining entire. Thus, the projectile breaks up in two fragments, yielding a three–body final state.

These results were confirmed by Padalino et al. [3] in the ^{27}Al(^{16}O, X) experiments performed at various incident energies between 72 and 125 MeV. Here, by kinematic considerations and the analysis of the inclusive energy spectra of reaction products, the authors also observe that the reaction mechanism is the projectile break–up leading to a two–body final state at lower energies and three–body final state at higher energies.

Comparing the ^{14}N+^{27}Al experiments at 62 and 116 MeV, it appears that in this energy range there is a transition from a two–body to a three–body final state process. It would, however, be interesting to test this tendency by performing ^{27}Al(^{14}N, X) experiments at other bombarding energies. Moreover, it is necessary to understand why the break–up calculations for the lighter fragments do not describe the experimental data well.

These discrepancies are not surprising if one thinks of the competitive presence of other mechanisms. Therefore, we studied the ^{27}Al(^{14}N, X) experiment at about 9 MeV/n bombarding energy at the U–240 Cyclotron Laboratory in Kiev, where the Petrascu et al. experiment [2] was performed earlier at about 8 MeV/n bombarding energy. In the present experiment, we analysed the inclusive spectra and angular distributions of the emitted nuclei lighter than projectile, and elestic scattering of ^{14}N.

2. *Experimental procedure*

The experiment was carried out using the 129.3 MeV ^{14}N^{+4} ion beam of the U–240 isochronous cyclotron at the Kiev Institute for Nuclear Research. The beam current intensity (about $10 - 20$ nA) was measured using a Faraday cup with a current integrator. A self–supported foil of ^{27}Al was used as a target. The Al thickness (400 μg cm^{-2}) was determined by proton backscattering at the Kharkov University electrostatic generator facility.

The reaction products were detected by two $\Delta E - E$ telescopes put at 18 cm from the target and subtending a solid angle of 0.9 msr. Each telescope consisted of a ΔE, totally depleted silicon surface barrier detector, and an E, silicon surface barrier detector, 30 μm and 1 mm thick, respectively. Another solid state detector, placed at $\theta_{lab} = 17.5^{\circ}$ with respect to the beam, was used as the monitor.

The calibration of the energy pulses from the two telescopes was obtained by:

(i) α–particles ($E_\alpha = 4.777$ MeV) emitted from a ^{226}Ra source put inside the scattering chamber, (ii) ^{14}N elastic scattering on ^{27}Al, ^{197}Au and ^{12}C targets at the 129.3 MeV beam energy. The results show a good agreement between the two calibration methods. The energy signals were recorded for each event, corrected for the energy losses in the target, stored and analysed off–line. Thus the identification of Z was good for all the observed reaction products while of A was satisfactory up to the carbon isotopes. The measurements were performed for ^{6,7}Li, ^{7,9}Be, ^{10,11}B, ^{12}C and ^{14}N isotopes in the θ_{lab} angular range between 5° and 30°.

The estimated error of 15% attributed to the absolute value of the differential cross–section reported in this work is related to the uncertainties in the targtet thickness, beam current integration and detector solid angles. The statistical error contribution, however, can be neglected.

3. Results and discussion

In order to normalize our experimental data, to obtain the optical model parameters and to deduce the reaction and fusion cross–sections, we measured the elastic scattering of the ^{14}N ions on ^{27}Al nuclei. The ^{14}N angular distribution analysis was performed by the GENOA code [4] in the framework of the optical model. Here, the optical parameters of the $^{16}\mathrm{O} + ^{28}\mathrm{Si}$ elastic scattering [5] were used as a starting point input. As a result of the fit, we obtain the six optical model parameters (see Table 1) for the $^{27}\mathrm{Al}(^{14}\mathrm{N}, ^{14}\mathrm{N})^{27}\mathrm{Al}$ scattering. In Table 1, we also report the σ_R total reaction cross–section (predicted by the optical model) and the σ_F fusion cross–section, obtained by the analysis of the differential cross–section for elastic scattering on the basis of a model developed by Pozdnyakov and Terenetskii [6]. We deduce $l_{gr} = 45\hbar$ from the σ_R reaction cross–section and $l_{cr} = 30\hbar$ from the σ_F fusion cross–section.

TABLE 1.
Optical model parameters for $^{14}\mathrm{N} + ^{27}\mathrm{Al}$ *elastic scattering.*

V (MeV)	r_v (fm)	a_v (fm)	W (MeV)	r_W (fm)	a_W (fm)	σ_R (mb)	σ_F (mb)
124.6	0.93	0.67	48.7	1.76	0.45	1609	780

The energy spectra of various isotopes from ^{6}Li to ^{12}C were measured, as already stated, in an angular range from 5° to 30° in the laboratory system. As an example, the above spectra observed at $\theta_{lab} = 10°$ are shown in Fig. 1. Here the nitrogen spectrum also appears. In this figure, two arrows indicate some characteristic energies: E_p is the energy of various reaction products calculated with the projectile velocity; E_c is the exit–channel Coulomb barrier calculated as

$$E_c = \frac{e^2 Z_1 Z_2}{r_0(A_1^{1/3} + A_2^{1/3})}, \tag{1}$$

where $Z_{1,2}$ and $A_{1,2}$ are the charge and mass numbers of the final nuclei, respectively, and r_0 parameter is 1.44 fm. The energy spectra of ^{10,11}B and ^{12}C show a broad structure and a fast slope on the right side, while the ones of the lighter isotopes tend to assume a bell shape. The maximum in these spectra is near the projectile velocity, and this supports a simple fragmentation process. The energy of all the peaks slightly decreases with the angle while the intensity of the only projectile–like fragments falls exponentially.

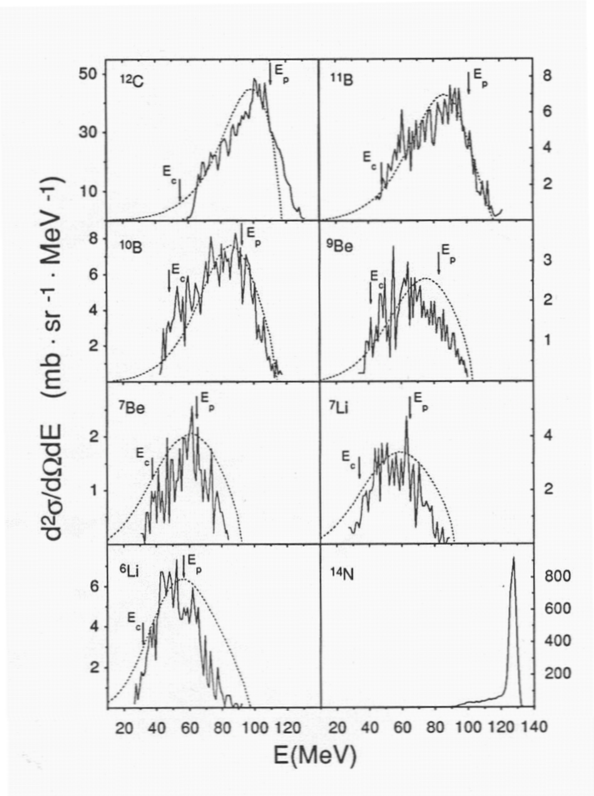

Fig. 1. Measured energy spectra (solid lines) at $\theta_{lab} = 10^\circ$ for various fragments produced in the 129.3 MeV ^{27}Al(^{14}N, X) *reaction. The dashed lines represent the three–body final state calculations. For the meaning of E_c and E_p see text.*

Moreover, as suggested by Petrascu et al. [2] and Padalino et al. [3], in Fig. 1 we also show by dashed lines three–body final state calculations obtained using a formalism based on the deuteron break–up model proposed by Serber [7], and developed by Matsuoka et al. [8] and Tabor et al. [1] for heavy–ion break–up. As one can see, our experimental spectra and the calculations are in line with the ones obtained by Petrascu et al. [2] in the sense that the agreement between the results and calculations is good for the projectile–like fragments and not so good for the lighter nuclei. A similar result also occurs for the other energy spectra that we measured in our experiment at various laboratory angles.

As far as the projectile–like fragments are concerned (where agreement between experiment and calculation is good), we cannot exclude the presence of other mechanisms like the deep–inelastic collision, whereas the above–mentioned difference for the lighter nuclei can be due to the presence of another mechanism that contributes to their formation together with the break–up without mass transfer. One of the possible emission processes is the evaporation from the ^{41}Ca compound nucleus after the fusion of ^{14}Na and ^{27}Al. At the 129.3 MeV incident energy, the composite system has an excitation energy of 106 MeV that corresponds to a nuclear temperature of 4.5 MeV. It could emit, however, sizeable amounts of lighter nuclei.

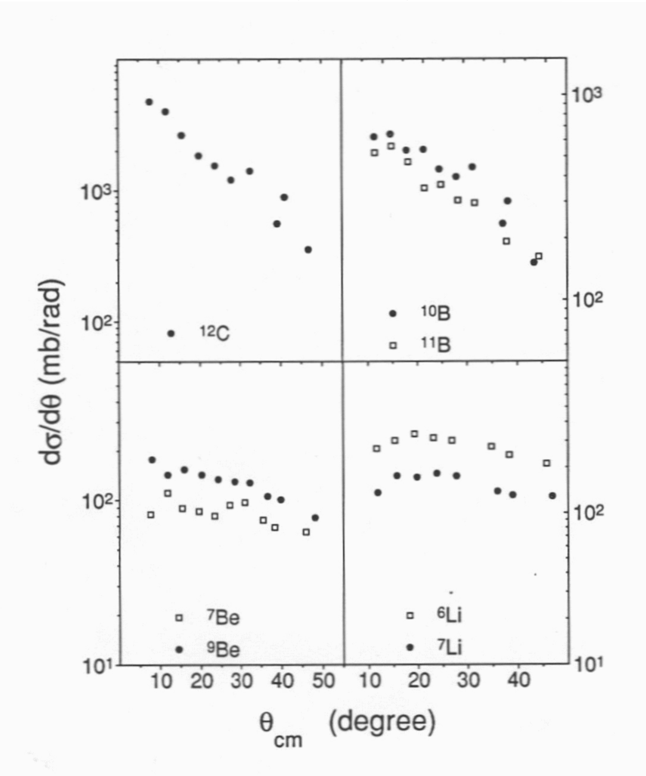

Fig. 2. Energy integrated angular distributions dσ/dθ *of various fragments produced in the* 129.3 MeV ^{27}Al(^{14}N, X) *reaction.*

In order to discover whether the above fragment formation in the ^{27}Al(^{14}N, X) reaction at E_{lab} = 129.3 MeV is also due to evaporation from ^{41}Ca compound nucleus, we analysed the dσ/dθ and dσ/dΩ distributions that we obtained for all the detected fragments. Figure 2 shows the energy integrated angular distribution dσ/dθ of the $^{6.7}$Li, ^{7,9}Be, ^{10,11}B and ^{12}C nuclei, produced by the above ^{27}Al(^{14}N, X) reaction at the 129.3 MeV energy. The distributions for the projectile–like nuclei are forward peaked, while for the Li and Be isotopes they are almost constant. It is evident that only the high slopes of the dσ/dθ distributions for ^{12}C and ^{10,11}B are compatible with a direct reaction mechanism.

To analyse the $d\sigma/d\Omega$ angular distribution, we used a classical model of rotating dinuclear system [9,10] with a mean lifetime τ, and angular velocity ω. In this model the distribution of the products is given by

$$\frac{d\sigma}{d\Omega} = \frac{c}{\sin\theta}\left[\exp\left(-\frac{\theta}{\alpha}\right) + \exp\left(-\frac{2\pi-\theta}{\alpha}\right)\right], \tag{2}$$

where c is a constant and $\alpha = \omega\tau$ the decay angle. The angular velocity can be calculated by the classical expression $\omega = \hbar l_i/\mu_i R_i^2$, where μ_i represents the reduced mass of the dinuclear system, l_i its angular momentum and R_i the distance between the two centers of the dinucleus. Theoretical calculations were made with $l_{gr} = 45\hbar$ and $R_i = 1.0(14^{1/3} + 27^{1/3})$ fm $= 5.41$ fm, assuming $\theta = 0°$ for the starting condition at $t = 0$. The curves obtained for all the detected fragments are reported in Fig. 3, while in Table 2 the values of the α–decay angles and of the corresponding lifetimes appear.

TABLE 2.
Decay angle and lifetime for the various fragments.

Detected fragment	α (deg)	τ ($\times 10^{-22}$ s)
^{6}Li	180	3.00
^{7}Li	180	3.00
^{7}Be	180	3.00
^{9}Be	60	1.00
^{10}B	40	0.67
^{11}B	30	0.50
^{12}C	18	0.30

As one can see, the values of τ for the production of carbon and boron are between 0.3×10^{-22} s and 0.67×10^{-22} s, as occurs for direct reactions [11]. This result is in line with the three–body final state analysis and the $d\sigma/d\theta$ distribution slopes. The angular distributions (going from the beryllium to the lithium isotopes) show, on the contrary, a growing tendency to approach $1/\sin\theta$ behaviour as in the case of the compound nucleus formation, and this result is in agreement with the almost constant angular distributions of Fig. 2 for the Li and Be isotopes. Consequently, the formation of these isotopes occurs by both the projectile break–up leading to a three–body final state reaction and the evaporation from the ^{41}Ca compound nucleus processes. Moreover, the σ_F/σ_R ratio at our energy is 0.48 and grows to about 0.85 at the energy (62 MeV) of the Tabor et al. experiment [1]. However, it is reasonable to think that at lower energies the lighter fragments are also produced by the evaporation process together with the projectile break–up leading to a two–body final state. Here, it is useful to remember that in this mass region the asymmetrical fission mechanism is competitive with the fusion–evaporation one [12]. Although it is not easy to evaluate these effects, it is the goal we are aiming at.

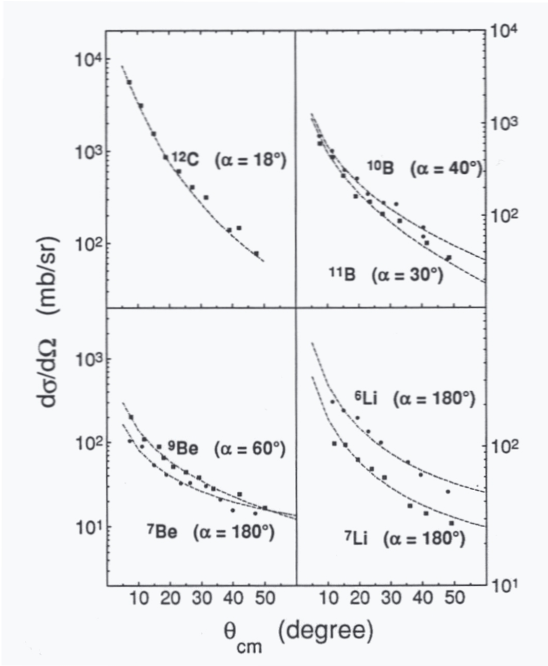

Fig. 3. $d\sigma/d\Omega$ *angular distributions of various fragments produced in the* 129.3 MeV ^{27}Al(^{14}N, X) *reaction. The dash–dotted lines represent the fits performed with Eq. (2) of the text. For each fit, the* α*–decay angle is reported.*

4. Summary and conclusions

The ejectiles, from Li to C, emitted in the 129.3 MeV ^{27}Al(^{14}N, X) experiment were studied by energy spectra, angular distributions and ^{14}N elastic scattering on the ^{27}Al target.

Regarding the boron and carbon isotopes, we can state that: (a) each energy spectrum is taken well into account by three–body final state calculations; (b) the $d\sigma/d\theta$ distributions are forward peaked; (c) the analysis of the $d\sigma/d\Omega$ angular distributions by the rotating dinuclear system shows lifetimes of $(0.3 - 0.67) \times 10^{-22}$ s, compatible with direct nuclear processes. All these results well support the hypothesis that the direct break–up mechanism appears strongly responsible for the production of ejectiles of mass close to the projectile.

On the contrary, for the lighter fragments: (a') the three–body final state calculations display a larger width in the energy spectra with respect to the experimental ones, (b') the $d\sigma/d\theta$ distributions show a flat shape, (c') the $d\sigma/d\Omega$ distributions show the tendency to approach $1/\sin\theta$. All this can be explained with the hypothesis that two mechanisms (direct, and emission from the compound nucleus) contribute to the lighter nucleus formation.

In conclusion, we can state that at higher energies the projectile break–up leading to a three–body final state reaction plays an important role in the formation of all the detected nuclei together with the evaporation (by ^{41}Ca compound nucleus) for the lighter fragments only, but contributions of other mechanisms could be present.

Acknowledgements

The authors whish to thank C. Beck, J. Wilczynski and V. V. Volkov for fruitful discussions and Yu. A. Pozdnyakov for the calculations about the fusion cross–section. Thanks are also due to O. A. Ponkratenko for projectile break–up calculations. This work was supported in part by the National Academy of Sciences of Ukraine and the Istituto Nazionale di Fisica Nucleare.

References

1) S. L. Tabor, L. C. Dennis and K. Abdo, Phys. Rev. C **24** (1981) 2552;
2) M. Petrascu, A. Isbasescu, I. Lazar, I. Mihai, H. Petrascu, A. T. Rudchik, V. A. Chernievski, O. A. Ponkratenko and V. A. Ziman, Z. Phys. A **345** (1993) 395;
3) S. J. Padalino, M. A. Putnam, J. A. Constable, T. G. De Clerck, L. C. Dennis, R. Zingarelli, R. Kline and K. Sartor, Phys. Rev. C **41** (1990) 594;
4) F. G. Perey, GENOA code as modified by L. W. Owen (unpublished);
5) J. Kramer, R. De Vries, D. Goldberg, M. Zissman and C. Maguire, Phys. Rev. C **14** (1976) 2158;
6) Yu. A. Pozdnyakov and K. O. Terenetskii, Sov. J. Nucl. Phys. **53** (1991) 249;
7) R. Serber, Phys. Rev. **72** (1947) 1008;
8) N. Matsuoka, A. Shimizu, K. Hosono, T. Saito, M. Kondo, H. Sakaguchi, Y. Toba, A. Goto and F. Ohtami, Nucl. Phys. A **311** (1978) 173;
9) C. K. Gelbke, C. Olmer, M. Buenerd, D. L. Hendrie, J. Mahoney, M. C. Mermaz and D. K. Scott, Phys. Rep. **42** (1978) 311;
10) J. Barette, P. Braun-Münzinger, C. K. Gelbke, H. E. Wegner, B. Zeidman, A. Gamp, H. C. Harney and Th. Walcher, Nucl. Phys. A **279** (1977) 125;
11) C. K. Gelbke, J. D. Garret, M. J. Le Vine and C. E. Thorn, Phys. Rev. C **14** (1976) 127;
12) C. Beck et al., Phys. Rev. C **54** (1996) 227.

MEHANIZMI REAKCIJA ^{27}Al(^{14}N, X) PRI ENERGIJI SNOPA OD 129,3 MeV

Reakcijom ^{14}N +^{27} Al odredili smo apsolutne vrijednosti diferencijalnih udarnih presjeka za tvorbu jezgri ^{6,7}Li, ^{7,9}Be, ^{10,11}B i ^{12}C pri energiji 129,3 MeV. Analiza inkluzivnih energijskih spektara i kutnih raspodjela pokazuje da se tvorba ugljikovih i borovih fragmenata može dobro opisati rascjepom upadne čestice koji vodi do tri tijela u konačnom stanju, dok su lakši fragmenti posljedica tog procesa i isparavanja iz složene jezgre.